

Quality analysis for precision metrology based on joint weak measurements without discarding readout data

Lupei Qin* and Xin-Qi Li†

Center for Joint Quantum Studies and Department of Physics, School of Science,
Tianjin University, Tianjin 300072, China

(Dated: July 11, 2022)

We present a theoretical analysis for the metrology quality of joint weak measurements (JWM), in close comparison with the weak-value-amplification (WVA) technique. We point out that the difference probability function employed in the JWM scheme cannot be used to calculate the signal-to-noise ratio (SNR) and Fisher information (FI). To overcome this difficulty, we propose an alternative formulation in terms of difference-combined stochastic variables, which makes all calculations well defined. Our results show that the SNR and FI of the JWM and WVA schemes are comparable and are bounded by the conventional scheme. In particular, we reveal that the JWM technique cannot reach the total FI in general, despite that all the readouts are collected without discarding. We also analyze the effect of technical noise, showing that the technical noise cannot be removed by the subtracting procedure in the JWM scheme.

I. INTRODUCTION

Based on the concept of quantum weak values (WVs) [1, 2] proposed by Aharonov, Albert and Vaidman (AAV), a novel precision metrology scheme termed as weak-value amplification (WVA) has been developed and received considerable attentions [3–23]. The WVA technique can lead to experimental sensitivity beyond the detector’s resolution. It allowed to use high power lasers with low power detectors while maintaining the optimal signal-to-noise ratio, and obtained the ultimate limit in deflection measurement with a large beam radius. The WVA technique can outperform conventional measurement in the presence of detector saturation and technical imperfections [18–20]. Also, it has been pointed out that the WVA technique can reduce the technical noise in some circumstances [3–5, 9–14], and can even utilize it to outperform standard measurement by several orders of magnitude by means of the imaginary weak-value measurements [9, 10, 12–14].

The WVA technique involves an essential procedure termed as post-selection, which discards a large portion of output data. However, it was proved that WVA technique can put almost all of the Fisher information about the parameter under estimation into the small portion of the remained data and show how this fact gives technical advantages [12–14]. Since such result is possible under an almost orthogonal pre- and post-selection procedure, which leads to ultra-small probability of post-selection, the WVA technique has caused controversial debates in literature [11–14, 24, 26–28, 35].

Taking a different strategy, the possibility of inducing anomalous amplification was proposed without discarding readout data, but instead using all the post-selection accepted (PSA) and post-selection rejected (PSR) data [29–33]. This proposal was referred to as joint-weak-measurement (JWM) scheme, since, in the presence of the post-selection classification, the system state and meter’s wavefunction are *jointly*

measured. However, being different from the WVA technique, where the intensity of the PSA data (in the so-called dark port) is very weak, in the JWM scheme, the intensities of the PSA and PSR data can be set *almost equal* and the difference between them reveals anomalous amplification [29, 30]. For this reason, this JWM technique was also dubbed *almost-balanced* weak values (ABWV) amplification [30–32]. In short, the ABWV technique utilizes two balanced weak values, rather than using the extremely unbalanced weak value as in the WVA scheme.

Existing theoretical analysis and experimental explorations revealed the main advantages of the ABWV technique as follows. (i) By subtracting the PSA and PSR readouts, a WVA-like response can be obtained in the *difference signal*. In experimental demonstrations, it was shown that the effect of signal amplification using the ABWV technique is more prominent than using the WVA technique [31–33]. (ii) Viewing that in the ABWV scheme all the readout data are collected without discarding, it was concluded that this scheme collects all of the Fisher information of the estimated parameter [29, 30]. (iii) Owing to subtracting, the ABWV technique permits the removal of systematic error, background noise, and fluctuations in alignments of the experimental setup [31–33]. In Ref. [32], it was shown that the ABWV technique offers on average a twice better signal-to-noise ratio (SNR) than WVA for measurements of linear velocities. (iv) In the ABWV scheme, prior information about the input state of the pointer is not required, since the sum of the PSA and PSR outputs can be used as well [30–32].

Viewing that the advantages summarized above were largely based on considerations of some external factors (e.g. limitations of specific experimental setups), in this work we present a comprehensive analysis for the intrinsic quality of the JWM technique in close comparison with the WVA scheme. The key feature of the JWM technique is using the difference signal, i.e., the difference of the PSA and PSR probability distribution functions (PDFs). We will show that using it to determine the signal amplification is well defined; however, calculation of variance and Fisher information (FI) based on the difference PDF is ill-defined, since the difference PDF is not positive-definite. To overcome this difficulty, we in-

*Electronic address: qinlupei@tju.edu.cn

†Electronic address: xinqi.li@tju.edu.cn

roduce the corresponding difference of combined stochastic variables (DCSVs), which makes the calculation of the signal amplification and its variance well defined. We are also able to define an effective FI by borrowing the Cramér-Rao bound (CRB) inequality. We find that, in general, i.e., with the number of the PSA results (N_1) unequal to that of the PSR results (N_2), the FI cannot be characterized by $F_{\text{tot}}^{(N)} = N_1 F_1 + N_2 F_2$ as highlighted in Refs. [29–32], where F_1 and F_2 are, respectively, the FI encoded in the PSA and PSR PDFs. In other words, we cannot say that all the FI is collected by JWM from its feature that all the readouts are collected without discarding data. Moreover, we analyze the effect of technical noise. Since the JWM technique is using a signal from the combination of two weak-values, the variance is the statistical sum of the variances of the PSA and PSR readouts. Therefore, the technical noise cannot be removed by the subtracting procedure in the JWM scheme. However, by performing the imaginary-WV measurement, the technical noise can be avoided or can be even utilized [12–14].

The paper is organized as follows. In Sec. II we reformulate the JWM scheme and point out that the difference probability function employed by the JWM technique cannot be used to calculate the SNR and FI. In Sec. III, in terms of DCSVs, an alternative formulation is proposed, which makes all calculations well defined and all comparisons reasonable. In Sec. IV we analyzed the effect of a few types of technical noise. Finally, we summarize the work with brief discussions in Sec. V.

II. JOINT-WEAK-MEASUREMENT SCHEME

Let us consider a two-state system coupled to a meter for JWM, as schematically shown in Fig. 1. The two-state system can correspond to the electron spin in the Stern-Gerlach setup, the photon polarization or which-path degree of freedom in quantum optics experiments, and many other possible realizations. In the Stern-Gerlach setup, the electron's trajectory is deflected when it passing through the inhomogeneous magnetic field. For quantum measurement in this setup [1, 2], the interaction between the system (spin) and meter can be described by $H' = \kappa P A$, with P the momentum operator and $A = \sigma_z$ the Pauli operator for the spin. In general, we assume that the spin of the electron is initially prepared in a quantum superposition

$$|i\rangle = c_1|1\rangle + c_2|2\rangle, \quad (1)$$

with $|1\rangle$ and $|2\rangle$ denoting the spin-up and spin-down states. The electron's transverse spatial wavefunction is assumed as a Gaussian

$$\Phi(x) = \frac{1}{(2\pi\sigma^2)^{1/4}} \exp\left[-\frac{x^2}{4\sigma^2}\right], \quad (2)$$

with σ the width of the wavepacket. After passing through the region of the inhomogeneous magnetic field, the entire state of the electron becomes entangled and is given by

$$|\Psi_T\rangle = c_1|1\rangle|\Phi_1\rangle + c_2|2\rangle|\Phi_2\rangle, \quad (3)$$

where the meter's wavefunctions read as

$$\Phi_j(x) = \frac{1}{(2\pi\sigma^2)^{1/4}} \exp\left[-\frac{(x - \bar{x}_j)^2}{4\sigma^2}\right]. \quad (4)$$

with $\bar{x}_{1,2} = \pm d$ the Gaussian centers shifted by the coupling interaction e^{-idPA} , where $d = \int_0^\tau dt \kappa = \kappa\tau$ and τ is the interacting time. The parameter d is what we are interested in and want to estimate through measuring the spatial wavefunction.

Let us first consider the conventional scheme of measurement, which does not involve measurement (post-selection) for the spin state. In this case, ignoring the spin state corresponds to tracing the spin degree of freedom, leaving thus the meter state given by

$$\rho_m = \text{Tr}_s(|\Psi_T\rangle\langle\Psi_T|) = |c_1|^2|\Phi_1\rangle\langle\Phi_1| + |c_2|^2|\Phi_2\rangle\langle\Phi_2|. \quad (5)$$

Based on this state, we have $\bar{x} = (|c_1|^2 - |c_2|^2)d$. It becomes clear that, for the conventional measurement (CM) without post-selection, the optimal choice is to prepare the spin in one of the basis states, e.g., in the spin-up state $|1\rangle$. This results in the largest signal $\bar{x} = d$. Meanwhile, the variance (uncertainty) is σ . One can thus define the so-called signal-to-noise ratio (SNR), $R_{\text{CM}}^{(1)} = d/\sigma$, to characterize the quality of measurement. If using N particles for the measurement (to estimate the parameter d), the estimate precision is characterized by

$$R_{\text{CM}}^{(N)} = \frac{d}{\sigma/\sqrt{N}}. \quad (6)$$

This SNR will be used as a standard for comparison with other measurement schemes, i.e., the WVA and JWM schemes to be discussed in this work.

Next, let us consider the WVA scheme, in the the AAV limit (weak enough d). It can be proved that after post-selection with $|f\rangle$ for the spin state, the meter's wavefunction is approximately given by [1, 2]

$$\tilde{\Phi}(x) = \frac{1}{(2\pi\sigma^2)^{1/4}} \exp\left[-\frac{(x - \text{Re}A_w^f d)^2}{4\sigma^2}\right], \quad (7)$$

where the AAV WV reads as

$$A_w^f = \frac{\langle f|A|i\rangle}{\langle f|i\rangle}. \quad (8)$$

For the task of parameter d estimation, we need the result of average of x . We see that, in the WVA scheme, the signal is enhanced as $\bar{x} = (\text{Re}A_w^f) d$, noting that the AAV WV A_w^f can be very large (strongly violating the bounds of the eigenvalues of A). Therefore, the SNR of the WVA measurement is characterized by $R_{\text{WVA}}^{(1)} = (\text{Re}A_w^f)d/\sigma$. When considering N particles used for the measurement but only N_1 particles survived in the post-selection, the SNR is given by

$$R_{\text{WVA}}^{(N)} = \frac{(\text{Re}A_w^f)d}{\sigma/\sqrt{N_1}}. \quad (9)$$

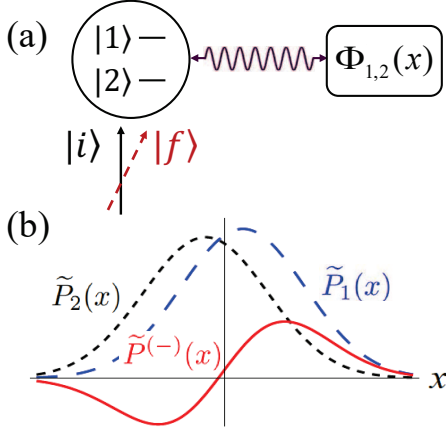


FIG. 1: (a) Schematic plot of a two-state system coupled to a meter in joint-weak-measurement (JWM) setup. The two-state system can correspond to the electron spin in the Stern-Gerlach setup, the photon polarization or which-path degree of freedom in quantum optics experiments, and many other possible realizations. The meter's wavefunction can be such as the transversal spatial wavefunction of an electron or a photon, which is deformed (shifted) from $\Phi(x)$ to $\Phi_{1,2}(x)$ by the system states $|1\rangle$ and $|2\rangle$, owing to measurement coupling interaction. In the WVA or JWM scheme, the system is initially prepared (preselected) in state $|i\rangle$ and post-selected using $|f\rangle$, while the meter's wavefunction is projectively measured to output the classical result of x . (b) The probability distribution functions (un-normalized) $\tilde{P}_1(x)$ and $\tilde{P}_2(x)$ of the PSA and PSR results of x . Their difference, $\tilde{P}^{(-)}(x)$, is the probability function employed in the JWM scheme to estimate the coupling interaction parameter, which can reveal the WVA-like signal with huge amplification. However, as schematically shown in the plot, $\tilde{P}^{(-)}(x)$ is not *positive-definite*, which cannot be used to calculate the distribution variance and Fisher information. This fundamental difficulty will be solved in this work by a technique of alternatively introducing difference-combined stochastic variables (DCSV), rather than using the ill-defined probability function $\tilde{P}^{(-)}(x)$.

From this result, despite that the signal is enhanced from d to $(\text{Re}A_w^f)d$, the SNR of the WVA scheme cannot be much improved as naively expected, since the uncertainty of estimation grows as well at the same time, owing to the small probability of successful post-selection, $p_f \simeq |\langle f|i\rangle|^2 \simeq N_1/N$ under the AAV limit. It can be proved [13] that the SNR of WVA scheme, $R_{\text{WVA}}^{(N)}$, can at most reach $R_{\text{CM}}^{(N)}$ of the conventional measurement, if using the same number of particles. It is just this trade-off consideration that has caused debates in literature [11–14, 24, 26–28, 35], despite that the WVA scheme does have some practical advantages as demonstrated by experiments [18–20].

Now, let us briefly reformulate the JWM scheme as follows. Beyond the AAV limit, the meter's wavefunctions associated with success and failure of the post-selection can be expressed as

$$\begin{aligned}\Phi_f(x) &= \langle f;x|\Psi_T\rangle = c_{1f}\Phi_1(x) + c_{2f}\Phi_2(x), \\ \Phi_{\bar{f}}(x) &= \langle \bar{f};x|\Psi_T\rangle = c_{1\bar{f}}\Phi_1(x) + c_{2\bar{f}}\Phi_2(x).\end{aligned}\quad (10)$$

Here, $|\bar{f}\rangle$ is orthogonal to the state $|f\rangle$ and the superposition

coefficients are updated as: $c_{1f} = \langle f|1\rangle c_1$ and $c_{2f} = \langle f|2\rangle c_2$, conditioned on success of the post-selection with state $|f\rangle$; $c_{1\bar{f}} = \langle \bar{f}|1\rangle c_1$ and $c_{2\bar{f}} = \langle \bar{f}|2\rangle c_2$, corresponding to failure of the post-selection. Respectively, the distribution probabilities of the measurement results are given by

$$\begin{aligned}\tilde{P}_1(x) &= |\Phi_f(x)|^2 \equiv p_f P_1(x), \\ \tilde{P}_2(x) &= |\Phi_{\bar{f}}(x)|^2 \equiv p_{\bar{f}} P_2(x).\end{aligned}\quad (11)$$

Here we introduced the normalized probability functions $P_1(x)$ and $P_2(x)$, and the probabilities of post-selection success and failure p_f and $p_{\bar{f}}$, which are also the normalization factors, i.e., $p_f = \int dx \tilde{P}_1(x)$ and $p_{\bar{f}} = \int dx \tilde{P}_2(x)$.

The JWM scheme suggests using the difference of the probability distribution functions (PDFs), i.e., $\tilde{P}^{(-)}(x) = \tilde{P}_1(x) - \tilde{P}_2(x)$, as a signal function from which the parameter is extracted. To gain a preliminary insight, and in more parallel to the experiments [30–33], let us consider the specific pre- and post-selection states $|i\rangle = (|1\rangle + |2\rangle)/\sqrt{2}$ and $|f\rangle = \cos\frac{\theta}{2}|1\rangle + \sin\frac{\theta}{2}|2\rangle$. The state orthogonal to the post-selection is $|\bar{f}\rangle = \sin\frac{\theta}{2}|1\rangle - \cos\frac{\theta}{2}|2\rangle$. Then, we obtain $\tilde{P}_1(x) = |\langle f;x|\Psi_T\rangle|^2$ and $\tilde{P}_2(x) = |\langle \bar{f};x|\Psi_T\rangle|^2$, where $|\Psi_T\rangle = (|1\rangle|\Phi_1\rangle + |2\rangle|\Phi_2\rangle)/\sqrt{2}$, based on Eq. (3). The difference probability function is further obtained as

$$\begin{aligned}\tilde{P}^{(-)}(x) &= \frac{1}{2} \left(\cos\theta e^{\frac{dx}{2\sigma^2}} - \cos\theta e^{-\frac{dx}{2\sigma^2}} + 2\sin\theta \right) P(x) \\ &\simeq \sin\theta \left(1 + \frac{d \cot\theta x}{\sigma^2} \right) P(x) \\ &\simeq \sin\theta P(x - d \cot\theta).\end{aligned}\quad (12)$$

Here we see that the shift of the wavepacket center is proportional to the parameter d under estimation. For small θ , $\cot\theta \simeq \frac{1}{\theta}$, this shift is anomalously amplified. In this case, one can check that the weak values $A_w^f = \langle f|A|i\rangle/\langle f|i\rangle$ and $A_w^{\bar{f}} = \langle \bar{f}|A|i\rangle/\langle \bar{f}|i\rangle$ are almost equal. For this reason, the JWM scheme was also referred to as ABWV technique [30–32].

To connect with experiment, let us consider using N particles. As schematically shown in Fig. 1, the PSA and PSR PDFs correspond to

$$\tilde{P}_1(x) = \frac{n_1(x)}{N} \quad \text{and} \quad \tilde{P}_2(x) = \frac{n_2(x)}{N}, \quad (13)$$

where $n_1(x)$ and $n_2(x)$ are the numbers of the PSA and PSR particles at point x . Then, one can define the *difference signal* as

$$P^{(-)}(x) = \frac{n_1(x) - n_2(x)}{N_1 - N_2}. \quad (14)$$

This is the normalized version of $\tilde{P}^{(-)}(x)$, with N_1 and N_2 the total PSA and PSR particle numbers. Using $P^{(-)}(x)$, one can estimate the parameter d from the average $\bar{x} = \int dx x P^{(-)}(x)$, which reads

$$\bar{x} = \langle x \rangle_f \left(\frac{\delta_1}{\delta_1 - \delta_2} \right) - \langle x \rangle_{\bar{f}} \left(\frac{\delta_2}{\delta_1 - \delta_2} \right), \quad (15)$$

where $\delta_1 = N_1/N$ and $\delta_2 = N_2/N$ correspond to the post-selection success and failure probabilities p_f and $p_{\bar{f}}$. In experiment, the conditional averages $\langle x \rangle_f$ and $\langle x \rangle_{\bar{f}}$ can be determined using the distribution functions $P_1(x) = n_1(x)/N_1$ and $P_2(x) = n_2(x)/N_2$; while in theory, they are computed using the normalized probability functions $P_1(x)$ and $P_2(x)$ given by Eq. (11). Then, making contact between the experimental and theoretical results of \bar{x} , one can extract (estimate) the value of the parameter d . The theoretical result becomes quite simple in the AAV limit, $\langle x \rangle_f = \text{Re}A_w^f d$ and $\langle x \rangle_{\bar{f}} = \text{Re}A_w^{\bar{f}} d$. Substituting them into Eq. (15), we know how to extract the parameter d from the experimental result of \bar{x} . Actually, in practice, even simpler method is possible [30–32]: using the collected data to fit the theoretical PDF (wavepacket profile) such as Eq. (12), one can extract the relevant parameters.

For arbitrary strength of measurement (beyond the AAV limit), using $P_1(x)$, one can straightforwardly obtain the WVA amplification factor as

$$\frac{\langle x \rangle_f}{d} = \frac{\text{Re}A_w^f}{1 + \mathcal{G}(|A_w^f|^2 - 1)} \equiv \frac{\text{Re}A_w^f}{\mathcal{M}_1}. \quad (16)$$

Here we introduced $\mathcal{G} = (1 - e^{-2g})/2$ and $g = (d/2\sigma)^2$, which is a suitable parameter to characterize the measurement strength. We also defined the modification factor \mathcal{M}_1 , which clearly reflects the modification effect to the AAV result. Using $P_2(x)$, similar result can be obtained for $\langle x \rangle_{\bar{f}}/d$, by only replacing A_w^f with $A_w^{\bar{f}}$ and denoting the modification factor as \mathcal{M}_2 .

The WVA scheme utilizes only the signal $\langle x \rangle_f$ in the first term of Eq. (15). Through proper choice of the post-selection state $|f\rangle$ (making it nearly orthogonal to $|i\rangle$), one can obtain an anomalous AAV WV, which corresponds to an anomalously large $\langle x \rangle_f$. This is the basic principle of WVA. From Eq. (15), the amplification principle of the JWM scheme is quite different: the anomalous amplification is owing to $\delta_1 \simeq \delta_2$. We know that the anomalous WV is deeply rooted in a nature of quantum interference [34]. For classical systems, it is impossible to realize such type of amplification. However, from Eq. (15), the amplification principle in the JWM scheme is seemingly applicable to measurements and statistics in classical systems. This might be an open and interesting problem worth further investigations.

In Fig. 2, we compare the amplification effects of the JWM and WVA techniques. For arbitrary strength of measurement, the JWM scheme can realize anomalously large amplification in the ABWV regime with $N_1 \simeq N_2$. However, for WVA, only at the AAV limit, it is possible to make the amplification factor anomalously large. With increase of the measurement strength, the amplification effect will be weakened.

Despite that the amplification is realized through the average of x governed by $P^{(-)}(x)$, this difference PDF is ill-defined, since it is not *positive-definite*, as illustrated in Fig. 1(b). This feature violates the *non-negative requirement* of any true probability functions. Using $P^{(-)}(x)$, one can easily examine that the distribution variance, or even the statistical average of x^2 , can be negative.

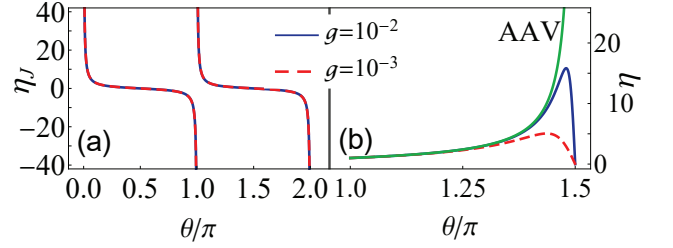


FIG. 2: Amplification factors of JWM in (a) and WVA in (b), defined by \bar{x}/d , by noting that d is the center’s shift of the meter wavefunction in conventional measurement. For JWM, the amplification effect is not sensitive to the measurement strength. For finite g beyond the AAV limit, the singular behavior can exist in the ABWV regime, i.e., $A_w^f \simeq A_w^{\bar{f}}$ when $\theta \rightarrow \pi$. In contrast, for WVA, the singular behavior of $\eta = \text{Re}A_w^f$ at the AAV limit when $\langle f|i \rangle \rightarrow 0$ and the anomalous amplification will be suppressed with increase of the measurement strength g .

We can also show that this ill-defined probability function will render the Crámer-Rao bound (CRB) inequality meaningless: it does not allow us to infer the estimate precision from the knowledge of Fisher information. Actually, in this case, the Fisher information itself is problematic. To be more general, let us consider an arbitrary parameter- λ -dependent probability function $P(x; \lambda)$, we have $\int dx P(x; \lambda)(x - \bar{x}) = 0$. Here, for brevity, we have denoted $P(x; \lambda)$ by $P(x)$ and \bar{x} is the average of x determined by $P(x; \lambda)$. Straightforwardly, making derivative with respect to the parameter λ , we have

$$\int dx \left(\frac{\partial P(x)}{\partial \lambda} \right) (x - \bar{x}) = \frac{\partial \bar{x}}{\partial \lambda}. \quad (17)$$

Further, applying the Cauchy-Schwarz inequality yields

$$\left(\frac{\partial \bar{x}}{\partial \lambda} \right)^2 \leq \mathcal{F} \int dx |P(x)| (x - \bar{x})^2, \quad (18)$$

where $\mathcal{F} = \int dx |P(x)| \left(\frac{1}{P(x)} \frac{\partial P(x)}{\partial \lambda} \right)^2$. For positive-definite probability function, every thing is perfect. That is, \mathcal{F} is the Fisher information which determines the upper bound of estimate precision through the above so-called CRB inequality.

For the ill-defined probability function $P^{(-)}(x)$, in principle, one can still compute the “Fisher information” using the above formula of \mathcal{F} . In some sense, it can reflect as well the sensitivity of the distribution function to the parameter under estimation. However, in the inequality Eq. (18), the “statistical variance” of x becomes completely meaningless. Based on the above analysis, we highly doubt the opinion that the JWM scheme collects all the information, owing to the feature that, unlike WVA, the JWM collects all the readout data of measurements [29, 30]. We also doubt the following quantitative characterization for the Fisher information collected by the JWM [30]:

$$F_{\text{tot}}^{(N)} = N_1 F_1 + N_2 F_2, \quad (19)$$

where the meaning of the particle numbers N_1 and N_2 is the

same as above, while F_1 and F_2 are the Fisher information associated with the PSA and PSR PDFs.

III. ALTERNATIVE FORMULATION: COMBINATION OF STOCHASTIC VARIABLES

Instead of the ill-defined probability distribution function $P^{(-)}(x)$, let us consider grouping the stochastic variables as follows

$$\begin{aligned} Y_1 &= \frac{1}{N_1} \sum_{j=1}^{N_1} x_j^{(f)}, \\ Y_2 &= \frac{1}{N_2} \sum_{k=1}^{N_2} x_k^{(\bar{f})}. \end{aligned} \quad (20)$$

This corresponds to the experiment using N particles, in which there are N_1 particles accepted by the post-selection, and N_2 particles rejected. In the first group, each stochastic variable obeys the statistics governed by $P_1(x)$ defined in Eq.(11), while in the second group each stochastic variable obeys the statistics governed by $P_2(x)$. Then, the difference signal exploited in the JWM scheme corresponds to the value of the following difference-combined stochastic variable (DCSV)

$$\begin{aligned} \hat{x} &= \left(\frac{N_1}{N_1 - N_2} \right) Y_1 - \left(\frac{N_2}{N_1 - N_2} \right) Y_2 \\ &\equiv \beta_1 Y_1 - \beta_2 Y_2. \end{aligned} \quad (21)$$

The ensemble average of \hat{x} reads as

$$E[\hat{x}] = \beta_1 \langle x \rangle_f - \beta_2 \langle x \rangle_{\bar{f}}, \quad (22)$$

which is the same as the \bar{x} given by the difference probability function $P^{(-)}(x)$. However, the variance of \hat{x}

$$\begin{aligned} D[\hat{x}] &= \beta_1^2 D[Y_1] + \beta_2^2 D[Y_2] \\ &= \beta_1^2 \left(\frac{\sigma_1^2}{N_1} \right) + \beta_2^2 \left(\frac{\sigma_2^2}{N_2} \right), \end{aligned} \quad (23)$$

is now well-defined and *positive-definite*, which properly characterizes the estimate precision. Here σ_1^2 and σ_2^2 are the variances of the single stochastic variables in the sub-ensembles defined by $P_1(x)$ and $P_2(x)$, respectively, which are introduced in Eq. (11). Under the AAV limit, both $P_1(x)$ and $P_2(x)$ are still Gaussian functions, with shifted centers of $\text{Re}A_w^f d$ and $\text{Re}A_w^{\bar{f}} d$ but keeping the widths $\sigma_1 = \sigma_2 = \sigma$ unchanged, as shown by Eq.(7). For finite strength of measurement, however, they are no longer Gaussian in general and may have different widths. Using $P_1(x)$ and $P_2(x)$ to calculate the variances, we obtain [14]

$$\begin{aligned} \sigma_1^2 &= \langle x^2 \rangle_f - (\langle x \rangle_f)^2 \\ &= \sigma^2 + d^2 \eta \left(\frac{|A_w^f|^2 + 1}{2\text{Re}A_w^f} - \eta \right). \end{aligned} \quad (24)$$

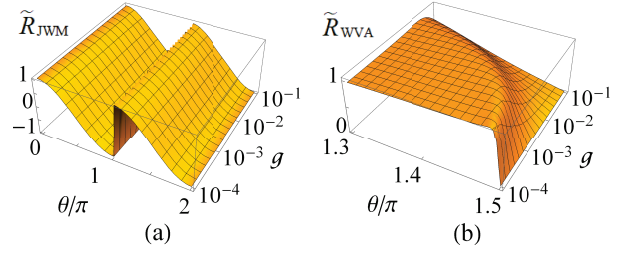


FIG. 3: Signal-to-noise ratio (SNR) of JWM in (a) and WVA in (b). Both results are scaled by the SNR of conventional measurement, $R_{\text{CM}}^{(N)} = \sqrt{Nd}/\sigma$, which is found to set an upper bound for the SNR of both JWM and WVA. For JWM, the SNR of anomalous amplification is not sensitive to g . In contrast, for WVA, the SNR associated with the anomalous amplification measurement is reduced with increase of the measurement strength g .

Here we introduced the amplification factor $\eta = |\langle x \rangle_f|/d$. Similar result of σ_2^2 can be obtained by replacing A_w^f with $A_w^{\bar{f}}$, and η by $\bar{\eta} = |\langle x \rangle_{\bar{f}}|/d$.

From the above results, we know that, with the signal being amplified, its fluctuation increases. Thus, a reasonable characterization to the quality of the JWM scheme is still the SNR

$$R_{\text{JWM}}^{(N)} = \frac{\beta_1 \langle x \rangle_f - \beta_2 \langle x \rangle_{\bar{f}}}{\sqrt{\beta_1^2 \left(\frac{\sigma_1^2}{N_1} \right) + \beta_2^2 \left(\frac{\sigma_2^2}{N_2} \right)}}. \quad (25)$$

In Fig. 3, we plot this SNR as a function of the post-selection angle θ and the measurement strength g , and compare it with the SNR of WVA. For both techniques, the maximum of the SNR are bounded by $\frac{d}{\sigma/\sqrt{N}}$, i.e., the SNR of conventional scheme. For the JWM technique, the maximum SNR can always be achieved in the ABWV regime with $N_1 \simeq N_2$. Similar as the amplification factor, this behavior of SNR is not sensitive to the measurement strength. In contrast, for WVA, we find that for small g , large range of post-selection can reach the maximum SNR. However, with the increase of g , this range is narrowed and gradually disappears.

As explained already, we cannot calculate the Fisher information by directly using the difference probability function $P^{(-)}(x)$. In the normal case (with positive-definite probability function), from the CRB inequality Eq. (18), we know that the SNR gives the lower bound of the Fisher information. Therefore, we may introduce an *effective* FI for the JWM scheme using the SNR of Eq. (25) as

$$F_{\text{JWM}}^{(N)} = \left[R_{\text{JWM}}^{(N)} \right]^2. \quad (26)$$

In Fig. 4, we compare this effective FI with the FI of the WVA scheme. In particular, we also compare them with the total FI given by Eq. (19). We see that, for very small g (in the AAV limit), the WVA technique can reach the FI of conventional measurement in the regime of near orthogonal post-selection (i.e., $\langle f|i \rangle \simeq 0$). The novel point in this context is that the post-selected small portion of measurement data contains almost the full information, which leads thus to a practical advantage in the presence of power saturation of the detectors.

With the increase of g (away from the AAV limit), we find that the WVA technique cannot reach the FI of conventional measurement. For the JWM scheme, in the ABWV regime with $N_1 \simeq N_2$, its effective FI can reach the FI of conventional measurement, regardless of the measurement strength g . The reason for this difference is as follows. The WVA scheme employs the anomalously large conditional average $\langle x \rangle_f$ as the amplified signal, which is rooted in a nature of quantum interference [34]. With the increase of g , this amplification effect will be reduced. On the contrary, the JWM scheme is free from any quantum interference effect.

An important observation here is that, except for the special post-selection with $N_1 \simeq N_2$, the effective FI of the JWM scheme drastically deviates from the $F_{\text{tot}}^{(N)}$ given by Eq. (19). Since the FI is usually used to characterize the estimate precision, it is not reasonable to regard $F_{\text{tot}}^{(N)}$ as the information collected in the JWM scheme, simply from the intuition that the N_1 and N_2 particles in both detectors are collected without data discarding. If using $F_{\text{tot}}^{(N)}$, the metrology precision will be overestimated in general.

We find that the optimal results are achieved in the ABWV regime with $N_1 \simeq N_2$. If the post-selection is not set in this regime, e.g., with $N_1 \simeq \beta N_2$, one may consider an asymmetric combination of the PSA and PSR data. In terms of probability distribution function, we have

$$P_{\beta}^{(-)}(x) = \frac{n_1(x) - \beta n_2(x)}{N_1 - \beta N_2}, \quad (27)$$

Similar to the symmetric combination scheme discussed above, we can construct the DCSV as

$$\begin{aligned} \hat{x}_{\beta} &= \left(\frac{N_1}{N_1 - \beta N_2} \right) Y_1 - \left(\frac{\beta N_2}{N_1 - \beta N_2} \right) Y_2 \\ &\equiv \tilde{\beta}_1 Y_1 - \tilde{\beta}_2 Y_2. \end{aligned} \quad (28)$$

Based on this DCSV, we can calculate the SNR and introduce the effective FI. One can easily check that, for both the amplification factor and the SNR (or the effective FI), the same optimal results can be achieved by post-selection satisfying $N_1 \simeq \beta N_2$, instead of the ABWV with $N_1 \simeq N_2$. This conclusion is valid as well for the results in the presence of technical noise, which is to be addressed in the following.

IV. EFFECT OF TECHNICAL NOISE

In practice, there may exist technical issues to cause extra noises, which are usually referred to as technical noises. In general, technical noises will increase the uncertainty of estimation, being thus harmful to precision metrology. For the real-WV measurement as shown by Eq. (7) at the AAV limit, it can be proved that the technical noise does not cause any shift of the signal (i.e., the average of $\langle x \rangle_f$), but does increase the variance of x . Therefore, the effect of the noise is similar as in the conventional measurement without post-selection. However, the story is quite different in the imaginary-WV measurement [14]. Given the form of the measurement interaction

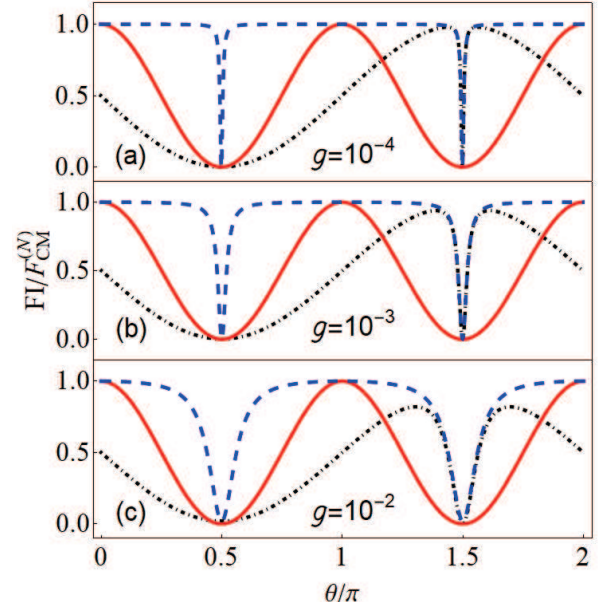


FIG. 4: Fisher information (FI) of JWM (solid red) and WVA (dash-dotted black), compared with the total FI $F_{\text{tot}}^{(N)} = N_1 F_1 + N_2 F_2$ (dashed blue). All results are scaled with the FI of conventional measurement, $F_{\text{CM}}^{(N)} = N(d/\sigma)^2$. For both the WVA at the AAV limit and the JWM in the ABWV regime, the FI can reach the result of conventional measurement. For most range of post-selection, $F_{\text{tot}}^{(N)}$ coincides also with $F_{\text{CM}}^{(N)}$. However, for JWM, except for the ABWV case with $N_1 \simeq N_2$, the FI drastically deviates from $F_{\text{tot}}^{(N)}$ which was conceived of the FI collected by the JWM technique [29, 30].

Hamiltonian $H' = \kappa PA$, the imaginary-WV measurement can be realized by performing measurement in the p basis, i.e., in the eigen-basis of the coupling operator P , while the real-WV measurement is performed in the conjugated x basis. Note also that, it is impossible to perform the conventional measurement (without post-selection) in the p -basis, since the average of p does not depend on the parameter d under estimation. Below, we present an investigation for the effect of technical noise in the JWM scheme.

Measurement in the x basis: x_0 noise.— Let us first consider the technical noise x_0 . The *joint probability* of getting x with the initial state $|i\rangle$ and passing the post-selection with $|f\rangle$, and as well with the specific noise x_0 , is given by

$$\Pr(f; x, x_0) = P_i(x - x_0) P_{x-x_0}(f) \Pr(x_0) / \mathcal{N}_f. \quad (29)$$

\mathcal{N}_f is a normalization factor. The first two probability functions read as $P_i(y) = |c_1|^2 |\Phi_1(y)|^2 + |c_2|^2 |\Phi_2(y)|^2$ and $P_y(f) = |\langle y; f | \Psi_T \rangle|^2$. Here we have denoted $x - x_0$ by y for brevity. The probability distribution of the noise is assumed to be Gaussian

$$\Pr(x_0) = \frac{1}{\sqrt{2\pi}J} e^{-x_0^2/2J^2}, \quad (30)$$

where J is the width of the noise distribution. Straightforwardly, one can compute the statistical average through

$\langle \bullet \rangle_f = \int dx_0 \int dx \langle \bullet \rangle \Pr(f; x, x_0)$. We obtain

$$\begin{aligned} \langle x \rangle_f &= \left(\frac{\text{Re} A_w^f}{\mathcal{M}_1} \right) d, \\ \langle x^2 \rangle_f &= \sigma^2 + J^2 + \left(\frac{\eta d^2}{2} \right) \left(\frac{1 + |A_w^f|^2}{\text{Re} A_w^f} \right). \end{aligned} \quad (31)$$

Accordingly, the variance is obtained as usual as $\sigma_{1J}^2 = \langle x^2 \rangle_f - (\langle x \rangle_f)^2$. The above results for the PSA data show that the signal shift is not affected by the noise, however, the variance is added by J^2 , as expected. Similar results of $\langle x \rangle_{\bar{f}}$, $\langle x^2 \rangle_{\bar{f}}$ and the variance σ_{2J}^2 for the PSR data can be obtained, by replacing A_w^f , η and \mathcal{M}_1 by $A_w^{\bar{f}}$, $\bar{\eta}$ and \mathcal{M}_2 , respectively. Here, we introduced $\bar{\eta} = |\langle x \rangle_{\bar{f}}|/d$. Substituting these results into Eq. (25), the SNR in the presence of the x_0 noise can be quantitatively computed. In this context, we may point out that the particle numbers N_1 and N_2 and the ratio parameters β_1 and β_2 in Eq. (25) are not affected by the technical noise. The basic conclusion for the effect of the noise is the same as for the conventional and WVA schemes: the technical noise will reduce the estimate precision, by adding extra uncertainty of J^2 as shown above.

Measurement in the p basis: x_0 and p_0 noises.— In order to avoid the influence of the technical noise and even possibly utilize it, let us consider further the so-called *imaginary* WV measurement. This can be realized by performing measurement in the p basis, i.e., in the eigen-basis of the coupling operator P in the measurement interaction Hamiltonian $H' = \kappa PA$. Therefore, we Fourier-transform the meter's wavefunctions from the x -representation to

$$\Phi_{1,2}(p) = \left(\frac{\pi}{2\sigma^2} \right)^{-1/4} \exp[-\sigma^2 p^2 \mp idp]. \quad (32)$$

Let us consider two types of noises. (i) The noise is introduced through x_0 , i.e., a random shift of the meter's wavefunction in the x basis. In this case, the meter's wavefunctions in the p basis can be reexpressed as

$$\Phi_{1,2}(p; x_0) = \left(\frac{\pi}{2\sigma^2} \right)^{-1/4} \exp[-\sigma^2 p^2 \mp idp - ix_0 p]. \quad (33)$$

As in the x -basis measurement, the x_0 noise satisfies the same Gaussian statistics of Eq. (30). (ii) The noise is introduced through a random p_0 shift of the p wavepacket. For a specific p_0 , the meter's wavefunctions are shifted from $\Phi_{1,2}(p)$ to

$$\Phi_{1,2}(p; p_0) = \left(\frac{\pi}{2\sigma^2} \right)^{-1/4} \exp[-\sigma^2 (p - p_0)^2 \mp idp] \quad (34)$$

As for the x_0 noise, the p_0 noise is assumed as well a Gaussian

$$\Pr(p_0) = \frac{1}{\sqrt{2\pi} J_p} e^{-p_0^2/2J_p^2}, \quad (35)$$

with J_p the width of the noise distribution.

For both types of noise, the joint probabilities are given by

$$\begin{aligned} \Pr(f; p, x_0) &= P_i(p, x_0) P_p(f) \Pr(x_0) / \mathcal{N}_f, \\ \Pr(f; p, p_0) &= P_i(p, p_0) P_p(f) \Pr(p_0) / \mathcal{N}_f. \end{aligned} \quad (36)$$

\mathcal{N}_f in each result is a normalization factor, and the first two probability functions read as $P_i(p) = |c_1|^2 |\Phi_1(p)|^2 + |c_2|^2 |\Phi_2(p)|^2$ and $P_p(f) = \langle f | \tilde{\rho}(p) | f \rangle$. Here, for brevity, we neglect the noise labels x_0 and p_0 . In both results, conditioned on the p outcome of measurement, the spin state is updated as $\tilde{\rho}_{12}(p) = \rho_{i12} e^{-i2dp}$, while the diagonal elements of the density matrix remain unchanged. This simply follows the result of $\tilde{\rho}(p) = |\tilde{\psi}(p)\rangle\langle\tilde{\psi}(p)|$, while the p -dependent spin state is obtained through $|\tilde{\psi}(p)\rangle = \langle p | \Psi_T \rangle = c_1 \Phi_1(p) |1\rangle + c_2 \Phi_2(p) |2\rangle$, based on Eq. (3).

For the type of x_0 noise, since $|\Phi_1(p; x_0)|^2$ and $|\Phi_2(p; x_0)|^2$ are free from the noise x_0 , then $P_i(p, x_0)$ does not depend on x_0 and averages of p and p^2 are free from x_0 . Therefore, an important conclusion is that the measurement in the p basis can eliminate the harmful effect of the x_0 noise. Note, however, that this advantage can be possible only by inserting the ingredient of post-selection measurement. One can check that, for the p basis measurement without post-selection (the conventional scheme), the 'signal' is zero. Using the joint probability $\Pr(f; p, x_0)$, the averages of p and p^2 for the PSA data can be obtained as

$$\begin{aligned} \langle p \rangle_f &= \left(\frac{\text{Im} A_w^f}{\mathcal{M}_1} \right) \left(\frac{d}{2\sigma^2} \right) e^{-d^2/2\sigma^2}, \\ \langle p^2 \rangle_f &= \frac{1}{4\sigma^2} + \left(\frac{|A_w^f|^2 - 1}{\mathcal{M}_1} \right) \left(\frac{d^2}{8\sigma^4} \right) e^{-d^2/2\sigma^2}. \end{aligned} \quad (37)$$

Precisely along the same line, using the joint probability $\Pr(\bar{f}; p, x_0)$ for the PSR data, the averages $\langle p \rangle_{\bar{f}}$ and $\langle p^2 \rangle_{\bar{f}}$ can be obtained.

For the type of p_0 noise, using the joint probability $\Pr(f; p, p_0)$, the averages of p and p^2 for the PSA data can be obtained as

$$\begin{aligned} \langle p \rangle_f &= \left(\frac{\text{Im} A_w^f}{\mathcal{M}_{1k}} \right) (2d/\tilde{\sigma}_J^2) e^{-2d^2/\tilde{\sigma}_J^2}, \\ \langle p^2 \rangle_f &= 1/\tilde{\sigma}_J^2 + \left(\frac{|A_w^f|^2 - 1}{\mathcal{M}_{1k}} \right) (2d^2/\tilde{\sigma}_J^4) e^{-2d^2/\tilde{\sigma}_J^2}. \end{aligned} \quad (38)$$

Here we introduced the second modification factor beyond the AAV limit, $\mathcal{M}_{1k} = 1 + K(|A_w^f|^2 - 1)$, with $K = (1 - e^{-2d^2/\tilde{\sigma}_J^2})/2$. We also introduced an effective width of uncertainty through

$$1/\tilde{\sigma}_J^2 = \frac{1}{4\sigma^2} + J_p^2. \quad (39)$$

Again, parallel results of $\langle p \rangle_{\bar{f}}$ and $\langle p^2 \rangle_{\bar{f}}$ for the PSR data can be obtained.

Knowing $\langle p \rangle_f$, $\langle p \rangle_{\bar{f}}$, and the variances σ_{1J}^2 and σ_{2J}^2 , applying Eq. (25) we can compute the SNR in the presence of the p_0 noise. From Eq. (25), we understand that the effect of the noise is basically rooted in the ratios $\langle p \rangle_f / \sigma_{1J}$ and $\langle p \rangle_{\bar{f}} / \sigma_{2J}$, while the more quantitative behaviors are modulated by the ratios β_1 and β_2 of the PSA and PSR readouts. In this context, we may remark that it is impossible to perform the conventional measurement (without post-selection) in the p -basis, since the average of p does not depend on the parameter d under estimation.

In Fig. 5 we compare the SNR of JWM with that of WVA, by varying the post-selection angle ϕ . For the JWM, we find

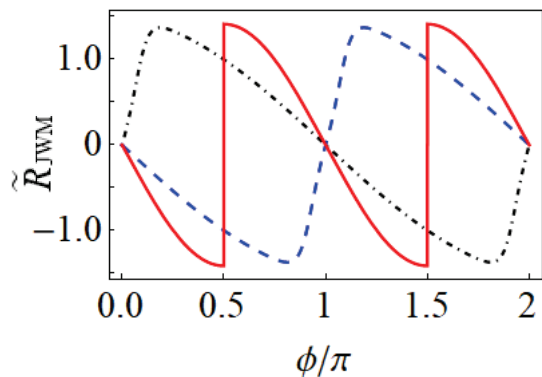


FIG. 5: SNR of imaginary weak-value measurement in the presence of technical noise (the p_0 -type, see main text for details). In order to generate imaginary weak values, with the initial system state $|i\rangle = (|1\rangle + |2\rangle)/\sqrt{2}$, the post-selected state is designed as $|f\rangle = (|1\rangle + e^{-i\phi}|2\rangle)/\sqrt{2}$. Plotted are the SNR of JWM (solid red), WVA post-selected by $|f\rangle$ (dashed blue) and WVA post-selected by $|\tilde{f}\rangle$ (dash-dotted black), respectively. The state $|\tilde{f}\rangle$ is orthogonal to $|f\rangle$. All the results are scaled by $R_{\text{CM}}^{(N)} = \sqrt{N}d/\sigma$ and arbitrary units with $d = 1$ are used. $J_p = 0.1d^{-1}$ and $g = (d/2\sigma)^2 = 10^{-2}$ are assumed for the noise strength and measurement strength. The results show that, in the presence of the p_0 -type noise, either the JWM or WVA technique can achieve estimate precision beyond the conventional measurement. This is the remarkable effect of “utilizing” technical noise. Also, the results show that the subtracting procedure of generating the *difference signal* cannot eliminate the technical noise considered in this work, unlike the situation considered in Refs. [31, 32].

that the ABWV regime with $N_1 \simeq N_2$ leads to the peaks at $\phi = \frac{\pi}{2}$ and $\frac{3\pi}{2}$, i.e., the discontinuous jumps, since we keep the sign of $N_1 - N_2$. We find also that the WVA measurement can reach similar maximum of SNR as well, at proper post-selection angle, which does not yet correspond to the post-selection nearly orthogonal to the initial state. Actually, we know that the SNR of JWM is related to the SNR of WVA through Eq. (25). This determines their behaviors as shown in Fig. 5. In particular, at $\phi = \frac{\pi}{2}$ and $\frac{3\pi}{2}$, the ABWV measurement holds equal SNR for the PSA and PSR results. In the experiment of Ref. [32], under equal conditions for both techniques (WVA and JWM), it was revealed that the JWM technique offered a twice better SNR than WVA. This might originate from the detecting limitations of the WVA, which make the WVA not working at optimal post-selection. Finally, we may remark that, as shown in Fig. 5 and by Eq. (25), the subtracting procedure of the JWM technique cannot remove the technical noise under consideration.

From Eq. (25), we know that the SNR of JWM is determined by the SNR of the individual weak-values. Therefore, similar as the imaginary WVA technique, the JWM scheme can utilize the technical noise as well, as shown in Fig. 6. In Fig. 6(a), we show that the SNR is enhanced with the increase of the noise (its distribution width J_p). By varying the post-selection angle ϕ , the overall behavior is displayed. Again, we find that the enhancement is most prominent at $\phi = \frac{\pi}{2}$ and $\frac{3\pi}{2}$, which correspond to the ABWV regime. In Fig. 6(b), we

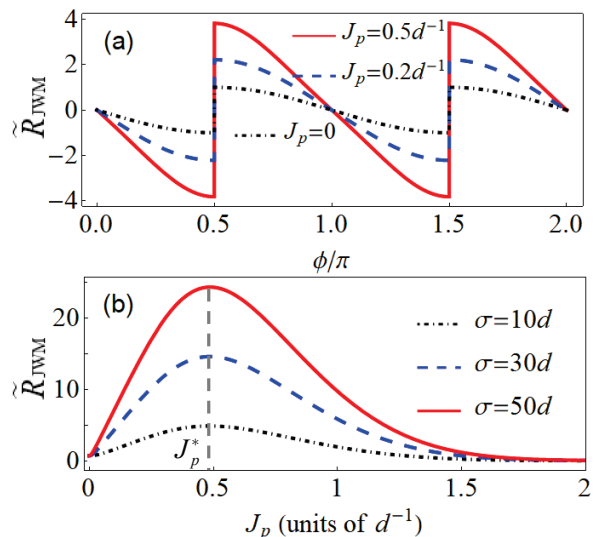


FIG. 6: Dependence of the p_0 noise strength. In (a) the complete range of post-selection is shown, while in (b) the post-selection state with $\phi = 3\pi/4$ is considered. The pre- and post-selected states $|i\rangle$ and $|f\rangle$ are the same as in Fig. 5. All the results of SNR of the JWM are scaled by $R_{\text{CM}}^{(N)} = \sqrt{N}d/\sigma$. In (a) the measurement strength $g = (d/2\sigma)^2 = 10^{-2}$ is assumed and in (b) the results of more strengths are shown. From (b), we find that the weaker the measurement strength is, the larger the noise-assisted enhancement of estimate precision is. However, this enhancement holds only for noise strength lower than the critical value J_p^* , as indicated by the vertical dashed line.

show the whole J_p dependence, which indicates that utilizing the noise is possible only for $J_p < J_p^*$. When $J_p > J_p^*$, the SNR will decrease with increase of the noise strength. Determination of the critical value J_p^* is referred to the detailed discussion in Ref. [14]

V. SUMMARY AND DISCUSSION

We have presented a theoretical analysis for the metrology quality of the JWM technique in close comparison with the WVA scheme. From the perspective of difference probability function, we reformulated the JWM scheme and revealed the *classical* origin of anomalous amplification, which is quite different from the *quantum* nature rooted in the WVA scheme. We pointed out that the difference probability function cannot be used to calculate the SNR and FI, being thus incapable of characterizing the estimate precision. To overcome this difficulty, we carried out an alternative formulation in terms of DCSVs, which makes all calculations well defined. Our results show that the SNR and FI of the JWM and WVA schemes are comparable and are bounded by the conventional scheme. However, both the JWM and WVA techniques do have their own technical advantages in the presence of technical imperfections, e.g., systematic errors, misalignment errors, and limitation of detector saturation. In particular, we revealed that the JWM scheme cannot reach the total FI in general, de-

spite that in this scheme all the readouts are collected without discarding. We also analyzed the effect of a few types of technical noise, showing that the technical noise cannot be removed by the subtracting procedure in the JWM scheme, but yet can be avoided or even utilized by performing imaginary-WVs measurement.

Based on our reformulation of the JWM, in particular Eqs. (14), (15), (21)-(23) and (25), we know that the amplification principle of the JWM scheme is quite different from the WVA. The amplification of the JWM technique is from a statistical trick, which is classical in essence. In contrast, the amplification of the WVA technique is rooted in a quantum interference effect [34]. Indeed, the effect of WVA becomes less prominent with the increase of measurement strength and should be impossible in classical systems. In contrast, the JWM technique seems applicable to classical precision metrology and

holds similar technical advantages in the presence of such as systematic errors, misalignment errors, and limitation of detector saturation. An initial study can be the model proposed in Ref. [35], where classical coin toss was assumed to generate the WVA-like response, which was yet negated later after more careful analysis [34]. We believe that the amplification effect of the JWM can be realized in this classical model.

Acknowledgements.— This work was supported by the National Key Research and Development Program of China (No. 2017YFA0303304) and the NNSF of China (Nos. 11675016, 11974011 & 61905174).

-
- [1] Y. Aharonov, D. Z. Albert, and L. Vaidman, *How the result of a measurement of a component of the spin of a spin-1/2 particle can turn out to be 100*, Phys. Rev. Lett. **60**, 1351 (1988).
- [2] Y. Aharonov and L. Vaidman, *Properties of a quantum system during the time interval between two measurements*, Phys. Rev. A **41**, 11 (1990).
- [3] O. Hosten and P. G. Kwiat, *Observation of the Spin Hall Effect of Light via weak measurements*, Science **319**, 787 (2008).
- [4] P. B. Dixon, D. J. Starling, A. N. Jordan, and J. C. Howell, *Ultrasensitive beam deflection measurement via interferometric weak value amplification*, Phys. Rev. Lett. **102**, 173601 (2009).
- [5] D. J. Starling, P. B. Dixon, A. N. Jordan, and J. C. Howell, *Optimizing the signal-to-noise ratio of a beam-deflection measurement with interferometric weak values*, Phys. Rev. A **80**, 041803 (2009).
- [6] D. J. Starling, P. B. Dixon, N. S. Williams, A. N. Jordan, and J. C. Howell, *Continuous phase amplification with a sagnac interferometer*, Phys. Rev. A **82**, 011802 (2010).
- [7] D. J. Starling, P. B. Dixon, A. N. Jordan, and J. C. Howell, *Precision frequency measurements with interferometric weak values*, Phys. Rev. A **82**, 063822 (2010).
- [8] X. Y. Xu, Y. Kedem, K. Sun, L. Vaidman, C. F. Li, and G. C. Guo, *Phase estimation with weak measurement using a white light source*, Phys. Rev. Lett. **111**, 033604 (2013).
- [9] N. Brunner and C. Simon, *Measuring small longitudinal phase shifts: weak measurements or standard interferometry?*, Phys. Rev. Lett. **105**, 010405 (2010).
- [10] A. Feizpour, X. Xingxing, and A. M. Steinberg, *Amplifying single-photon nonlinearity using weak measurements*, Phys. Rev. Lett. **107**, 133603 (2011).
- [11] A. Nishizawa, K. Nakamura, and M. K. Fujimoto, *Weak value amplification in a shot-noise-limited interferometer*, Phys. Rev. A **85**, 062108 (2012).
- [12] Y. Kedem, *Using technical noise to increase the signal-to-noise ratio of measurements via imaginary weak values*, Phys. Rev. A **85**, 060102(R) (2012).
- [13] A. N. Jordan, J. Martinez-Rincon, and J. C. Howell, *Technical advantages for weak-value amplification: when less is more*, Phys. Rev. X **4**, 011031 (2014).
- [14] J. Ren, L. Qin, W. Feng, and X. Q. Li, *Weak-value-amplification analysis beyond the Aharonov-Albert-Vaidman limit*, Phys. Rev. A **102**, 042601 (2020).
- [15] S. Pang and T. A. Brun, *Improving the Precision of Weak Measurements by Postselection Measurement*, Phys. Rev. Lett. **115**, 120401 (2015).
- [16] S. Pang, J. R. G. Alonso, T. A. Brun, and A. N. Jordan, *Protecting weak measurements against systematic errors*, Phys. Rev. A **94**, 012329 (2016).
- [17] J. Martínez-Rincón, C. A. Mullarkey, G. I. Viza, W. T. Liu, and J. C. Howell, *Ultra sensitive inverse weak-value tilt meter*, Opt. Lett. **42**, 2479 (2017).
- [18] J. Harris, R. W. Boyd, and J. S. Lundeen, *Weak Value Amplification Can Outperform Conventional Measurement in the Presence of Detector Saturation*, Phys. Rev. Lett. **118** 070802 (2017).
- [19] J. Huang, Y. Li, C. Fang, H. Li, and G. Zeng, *Toward Ultra-high Sensitivity in Weak Value Amplification*, Phys. Rev. A **100**, 012109 (2019).
- [20] L. Xu, Z. Liu, A. Datta, G. C. Knee, J. S. Lundeen, Y. Lu, and L. Zhang, *Approaching Quantum-Limited Metrology with Imperfect Detectors by Using Weak-Value Amplification*, Phys. Rev. Lett. **125**, 080501 (2020).
- [21] J. Dressel, K. Lyons, A. N. Jordan, T. M. Graham, and P. G. Kwiat, *Strengthening weak value amplification with recycled photons*, Phys. Rev. A **88**, 023821 (2013).
- [22] S. A. Haine, S. S. Szigeti, M. D. Lang, and C. M. Caves, *Heisenberg-limited metrology with information recycling*, Phys. Rev. A **91**, 041802 (2015).
- [23] C. Krafczyk, A. N. Jordan, M. E. Goggin, and P. G. Kwiat, *Enhanced weak-value amplification via photon recycling*, Phys. Rev. Lett. **126**, 220801 (2021).
- [24] S. Tanaka and N. Yamamoto, *Information amplification via postselection: a parameter-estimation perspective*, Phys. Rev. A **88**, 042116 (2013).
- [25] C. Ferrie and J. Combes, *Weak value amplification is suboptimal for estimation and detection*, Phys. Rev. Lett. **112**, 040406 (2014).
- [26] G. C. Knee and E. M. Gauger, *When amplification with weak values fails to suppress technical noise*, Phys. Rev. X **4**, 011032 (2014).
- [27] L. Zhang, A. Datta, and I. Walmsley, *Precision Metrology Using Weak Measurements*, Phys. Rev. Lett. **114**, 210801 (2015).
- [28] A. N. Jordan, J. Tollaksen, J. E. Troupe, J. Dressel, Y. Aharonov, *Heisenberg scaling with weak measurement: a*

- quantum state discrimination point of view*, Quantum Stud.: Math. Found. **2**, 5 (2015).
- [29] G. Strübi and C. Bruder, *Measuring Ultrasmall Time Delays of Light by Joint Weak Measurements*, Phys. Rev. Lett. **110**, 083605 (2013).
- [30] J. Martínez-Rincón, W.-T. Liu, G. I. Viza, and J. C. Howell, *Can Anomalous Amplification Be Attained without Postselection?* Phys. Rev. Lett. **116**, 100803 (2016).
- [31] W.-T. Liu, J. Martínez-Rincón, G. I. Viza, and J. C. Howell, *Anomalous amplification of a homodyne signal via almost-balanced weak values*, Opt. Lett. **42**, 903 (2017).
- [32] J. Martínez-Rincón, Z. Chen, and J. C. Howell, *Practical advantages of almost-balanced-weak-value metrological techniques*, Phys. Rev. A **95**, 063804 (2017).
- [33] C. Fang, J.-Z. Huang, Y. Yu, Q.-Z. Li, and G. Zeng, *Ultra-small phase estimation via weak measurement with postselection: A comparison of joint weak measurement and weak value amplification*, J. Phys. B: At. Mol. Opt. Phys. **49**, 175501 (2016).
- [34] L. Qin, W. Feng, and X. Q. Li, *Simple understanding of quantum weak values*, Sci. Rep. **6**, 20286 (2016).
- [35] C. Ferrie and J. Combes, *How the result of a single coin toss can turn out to be 100 heads*, Phys. Rev. Lett. **113**, 120404 (2014).